Design of an Extreme Ultraviolet Spectrometer Suite to Characterize Rapidly Heated Solid Matter

Introduction

Solid-density hot plasmas can be created by using a high-intensity laser incident on a solid metal foil.[1] Following irradiation by the high-intensity laser, the target heats in a matter of picoseconds. Electrons in the laser's focal spot are rapidly energized and confined to a target volume by a sheath set up around the target. The fast electrons thermalize through collisional and noncollisional processes that occur much faster than the hydrodynamic expansion time scale. This makes it possible to heat the target to high temperatures before the onset of hydrodynamic motion, allowing one to measure the hot plasma in a pre-expanded state. These conditions form a platform for measuring intrinsic material properties such as the equation of state (EOS) of high-energy-density (HED) matter.

X-ray and ultraviolet spectroscopy have been used to extract information about the temperature and density evolution of hot, solid-density targets in a variety of conditions. A new extreme ultraviolet (XUV) spectrometer has been built to make temperature measurements that provide complementary information to higher-energy spectroscopic observations (e.g., K_α-line spectroscopy or thermal-line radiation) of the mass-averaged temperature. The XUV radiation is highly localized to the surface of the promptly heated material before expansion. The early-time heating dynamics of the target are important to understand for future off-Hugioniot EOS measurements.

Spectrometer Layout

Figure 147.39 provides a schematic overview of the spectrometer and camera layout. A high-throughput XUV spectrometer was realized using a grazing-incidence toroidal reflector and a variable line-space grating.[2] A precision-cut 100-mm × 2-mm slit[3] is held close to the target with a re-entrant nose cone. All direct lines of sight between the target interaction and the charge-coupled–device (CCD) detector are shielded by a minimum of 6-mm tungsten to minimize the noise from hard x-ray hits on the camera. Two limited apertures inside the spectrometer serve to limit stray light. The spectrometer consists of a modular front section that can be mounted to a scientific CCD camera (Spectral Instruments SI-800), an image plate, or an x-ray streak camera. Two identical spectrometers have been built for simultaneous time-averaged and time-resolved XUV emission studies.

The spectrometer consists of a 450-lines/mm, variable line space grating[2] and a toroidal mirror,[2] which images the spectrum to a flat-field detector located outside the target chamber. Both the grating and mirror operate at a grazing angle of 7.5°. The mirror and the detector plane are located 190 mm and 570 mm from the laser focus, respectively. The view angle for both spectrometers is 45° with respect to the optical axis of the incident laser. The solid angle of both spectrometers is limited by the toroidal reflector and is 3×10^{-3} sr; the spectrometer

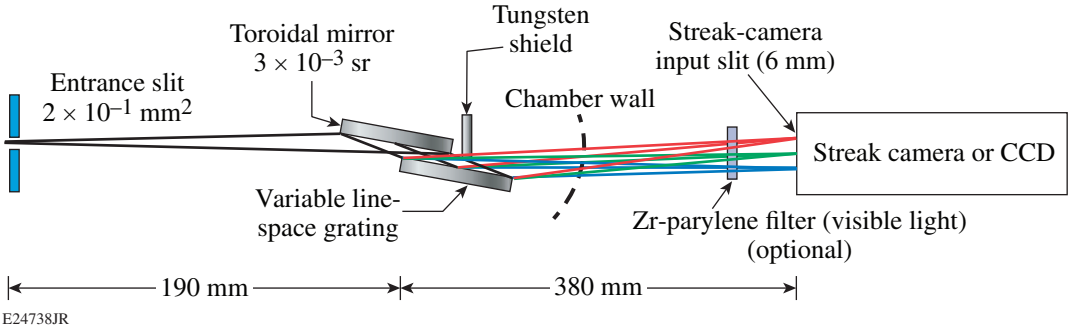

Figure 147.39
Schematic diagram of the extreme ultraviolet (XUV) flat-field spectrometer. CCD: charge-coupled device.

has a magnification of 3, giving a field of view of ~500 μm in the target plane. A ray-trace model of the spectrometer was implemented in the code *FRED* to simulate the optical performance of the spectrometer.[4] The simulation predicts a spectral resolution of 0.1-nm full width at half maximum (FWHM) at 12.5 nm.

Figure 147.40 shows a schematic of the spectrometer with the top sectioned for clarity. The slit aperture is held in place with a threaded cap on the front nose cone. The cap may be removed to replace or inspect the aperture slit between shots. A pointer can be attached to the nose cone to aid in spectrometer alignment on the target chamber's viewing system. The cone-shaped projection on the front of the spectrometer body limits blast material from the experiment from depositing into the spectrometer or onto the fine-adjust knobs of the grating carriage. The toroidal mirror is pinned in place on a custom kinematic mounting. The grating can be rotated ±3° about two axes to allow for pointing and spectral window adjustment. The actuators for the tip/tilt adjustment pass through to the front end to allow for adjustment between shots when the chamber is vent cycled. The outer casing of the spectrometer is vented with sintered plugs to allow for venting during pump out. The tungsten line-of-sight (LOS) shield forms the rear panel on the enclosure and provides a limited aperture for the spectrum to pass through to the detector.

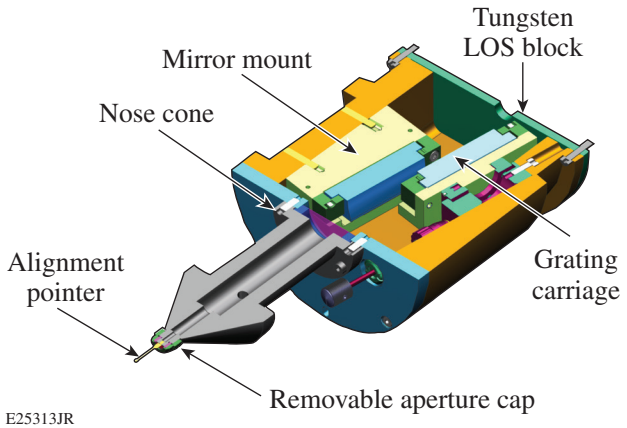

Figure 147.40
Schematic of the re-entrant spectrometer's front end. LOS: line of sight.

Experiment

An experiment to validate the spectrometer performance and to measure short-pulse heating was conducted on LLE's Multi-Terawatt (MTW) Laser System.[5,6] The experimental setup is shown schematically in Fig. 147.41. A 100 × 100 × 3-μm Al foil was irradiated with 7±1 J of 527-nm light in a 1-ps pulse with a contrast ratio of ~10^{14}. The contrast is estimated by measuring the pulse contrast at the fundamental frequency and calculated for the second-harmonic process.[7] The laser delivered a focus with 80% of the energy contained into a 10-μm spot when measured on a low-power shot. The on-target intensity was ~3×10^{18} W/cm^2. The XUV photocathode on the streak camera was a 200-Å gold layer flash coated onto a 0.5-μm parylene base layer. The full photocathode slit measures 60 mm × 200 μm wide but typically only the central 6 mm × 50 μm of the slit is used when the camera is set for best temporal focusing.

Data Analysis

Figure 147.42 shows a time-integrated spectrum taken with the spectrometer onto a FUJI TR image-plate (IP) detector. The spectrum occupies ~1 mm on the IP detector in the direction opposite the spectrum; the values shown are the summed values from the scanned data. The IP was scanned at a resolution of 50 μm and a sensitivity level of 10,000. Several atomic transition lines from Al III, IV, and V ions are visible superimposed on the continuum emission in this time-integrated shot. The strongest lines observed are listed in Table 147.IV; these values were obtained from the National Institute of Standards and Technology (NIST)[8] wavelength database. The Al III transition was observed in absorption

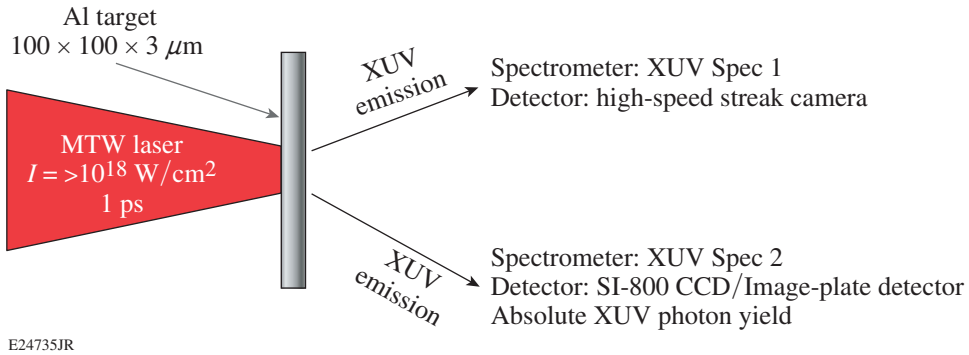

Figure 147.41
Schematic diagram of the experimental setup. MTW: Multi-Terawatt.

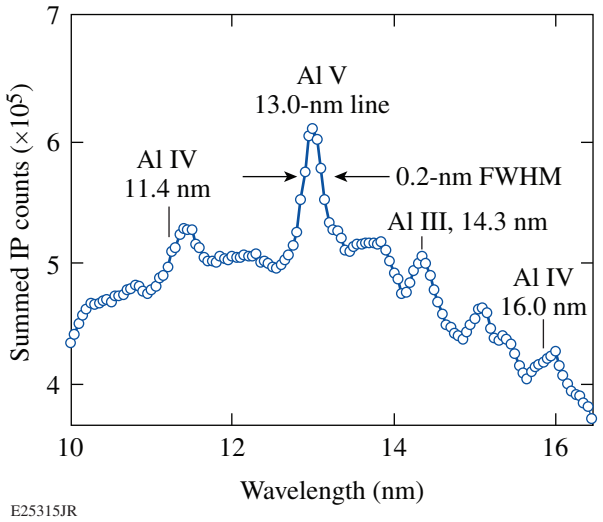

Figure 147.42
Spectrum acquired on a 7-J, 1-ps laser shot onto a 100 × 100 × 3-μm Al target. The spectrometer resolution was measured to be 0.2-nm full width at half maximum (FWHM).

Table 147.IV: Aluminum atomic spectral lines identified in a short-pulse, heated aluminum target.

Ion	Experimental data (nm)	Reference data[8] (nm)	Relative intensity[8]	Oscillator strength[8]
Al IV	11.4±0.2	11.646	250	0.332
Al V	13.0±0.2	13.0847	1000	0.175
Al IV	16.0±0.2	16.169	700	0.017
Al III	14.3±0.2	14.395	—	—

only and no tabular data exist for the line strength or relative intensity. Additionally, the spectrometer resolution at 13.0 nm was measured to be 0.2-nm FWHM. The Al line at 13.0 nm is a doublet (13.0 and 13.1 nm) and some broadening of the peak is expected; however, the resolution at this wavelength is consistent with simulation predictions (0.2 nm versus 0.1 nm). The peak at 15.1 nm is likely O IV ions from an oxide layer on the surface of the target.

Figure 147.43 compares a time-resolved spectrum recorded on an MTW shot and a synthetic spectrum. For this comparison we used the collisional-radiative code *Spect3D* to compute the emergent radiation from the radiation–hydrodynamics simulation.[9] The XUV atomic model in *Spect3D* includes all ionization stages and excited-state energy levels. A radiation–hydrodynamics simulation was run with parameters closely tied to the experiment.[10] In the simulation, a uniform energy density corresponding to the electron deposition was applied to the solid metal target and allowed to freely expand. The target temperature was initialized in the simulation at 100 eV. The emission is assumed to be in local thermodynamic equilibrium. In the time period of interest, the emission is predicted to be dominated by a smooth continuum with all the atomic transitions dissolved into the continuum. Later in time, the strongest emissions from ground-state transitions are observed. Previous inferences of temperature from the emission in this region have shown significant departures between the temperature observed in the continuum and electronic line ratios in time-integrated XUV spectrum measurements.[11,12] The streaked data here show that the continuum and line radiation occur at substantially different times in the expansion. This may explain the discrepancy between the temperature inferred from line emission and continuum emission.

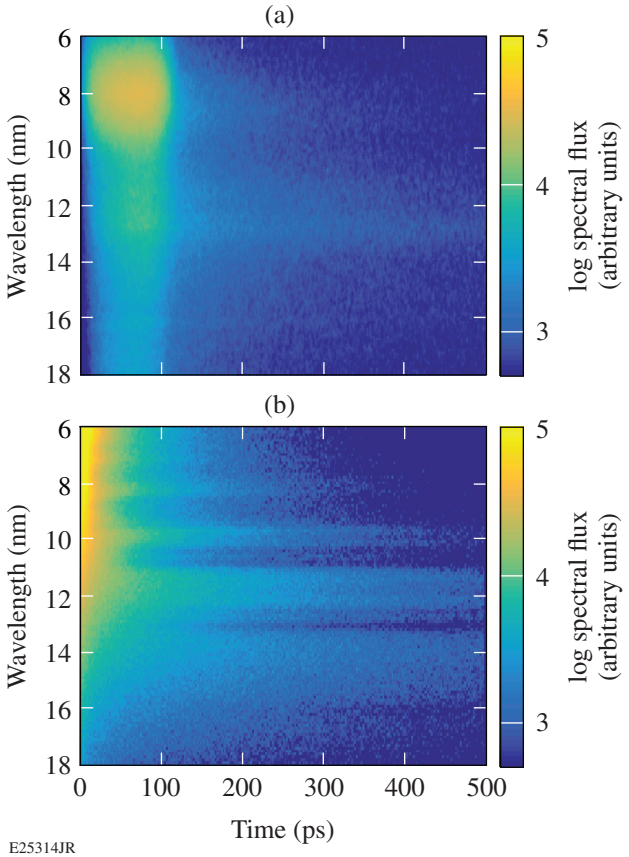

Figure 147.43
Comparison of (a) streaked XUV data and (b) simulation.

The streaked spectra can be corrected for the wavelength-dependent photocathode sensitivity. The first step is to take a photometric calibration of the streaked spectrometer. A method similar to those described in Ref. 13 will be implemented when correcting the raw streak-camera data. During a shot, the streaked and time-integrated spectrometer acquires a spectrum. The spectrum captured, on a calibrated IP detector, is then compared to a streaked spectrum summed in the temporal direction. Grating efficiency as a function of wavelength will be corrected using a rigorous coupled-wave theory code, taking into account the groove shape, depth, and metal reflectivity.[14]

Conclusion

A spectrometer capable of measuring the time-resolved XUV emission of a rapidly heated metal target has been designed and implemented. The spectrometer has a measured resolution of 0.2 nm at a design wavelength of 13 nm. The time-resolved spectra show reasonable agreement with radiation–hydrodynamic simulations. Future experiments will further explore the surface-temperature dynamics of these targets in a variety of metals.

ACKNOWLEDGEMENT

This material is based upon work supported by the Department of Energy National Nuclear Security Administration under Award Number DE-NA0001944, the University of Rochester, and the New York State Energy Research and Development Authority. This work was performed under the auspices of the U.S. Department of Energy, Office of Science, Office of Fusion Energy Sciences Award Number DE-SC-0012317.

REFERENCES

1. R. G. Evans *et al.*, Appl. Phys. Lett. **86**, 191505 (2005).
2. HORIBA Scientific, Edison, NJ 08820-3097.
3. National Aperture, Inc. Salem, NH 03079.
4. *FRED*, Photon Engineering, LLC, Tucson, AZ 85711 http://www.photonengr.com/software (1 June 2016).
5. V. Bagnoud, I. A. Begishev, M. J. Guardalben, J. Puth, and J. D. Zuegel, Opt. Lett. **30**, 1843 (2005).
6. C. Dorrer, I. A. Begishev, A. V. Okishev, and J. D. Zuegel, Opt. Lett. **32**, 2143 (2007).
7. I. A. Begishev, C. R. Stillman, S. T. Ivancic, S.-W. Bahk, R. Cuffney, C. Mileham, P. M. Nilson, D. H. Froula, J. D. Zuegel, and J. Bromage, "Efficient Second-Harmonic Generation of Large-Aperture Multi-Terawatt Hybrid Nd:Laser Subpicosecond Pulses for Laser–Matter Interactions," to be submitted to Applied Physics.
8. NIST Atomic Spectra Database, NIST Standard Reference Database #78, Version 5, see http://www.nist.gov/pml/data/asd.cfm (1 June 2016).
9. J. J. MacFarlane *et al*., High Energy Density Phys. **3**, 181 (2007).
10. J. Delettrez, R. Epstein, M. C. Richardson, P. A. Jaanimagi, and B. L. Henke, Phys. Rev. A **36**, 3926 (1987).
11. T. Ma *et al*., Rev. Sci. Instrum. **79**, 10E312 (2008).
12. U. Zastrau *et al*., Phys. Rev. E **78**, 066406 (2008).
13. R. Florido, R. C. Mancini, T. Nagayama, R. Tommasini, J. A. Delettrez, S. P. Regan, V. A. Smalyuk, R. Rodríguez, and J. M. Gil, High Energy Density Phys. **6**, 70 (2010).
14. L. Li *et al*., Appl. Opt. **38**, 304 (1999).